nature nanotechnology

SUPPLEMENTARY INFORMATION

DOI: 10.1038/NNANO.2014.296

All-electric all-semiconductor spin field-effect transistors

Pojen Chuang,† Sheng-Chin Ho,† L. W. Smith, F. Sfigakis, M. Pepper, Chin-Hung Chen, Ju-Chun Fan, J. P. Griffiths, I. Farrer, H. E. Beere, G. A. C. Jones, D. A. Ritchie & T.-M. Chen*

† These authors contributed equally to this work.

*To whom correspondence should be addressed; E-mail: tmchen@mail.ncku.edu.tw.

Supplementary Section 1. QPC conductance

All the QPCs employed in the spin FET devices display one-dimensional (1D) conductance quantization, as shown in Supplementary Fig. 1a. Although the introduction of the SO coupling results in two spin-polarized 1D subbands shifted horizontally along the k_x axis (Supplementary Fig. 1b), the QPC conductance quantization remains the same as the spin degenerate case without SO coupling[21,25], because the edge of the two spin-polarized 1D subbands are still at the same energy, simultaneously passing through the Fermi level such that the conductance changes by $2e^2/h$. This is consistent with our measurement in which no major difference in quantized conductance was observed between traces at $\Delta V_g = 0$ and $\Delta V_g = -3$ V.

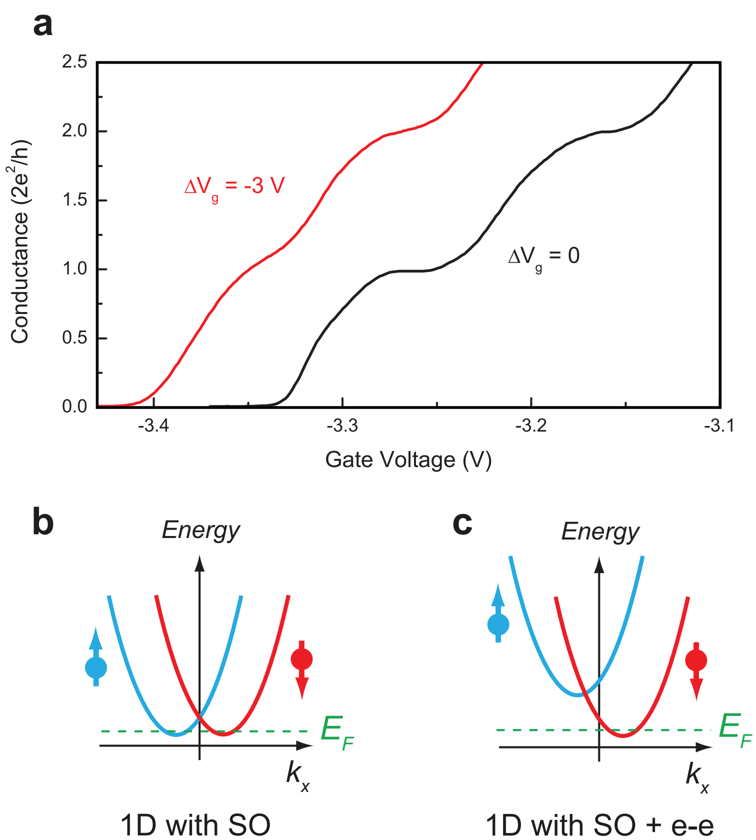

Supplementary Fig. 1: **QPC conductance.** **a**, The QPC conductance as a function of common-mode gate voltage measured for symmetric ($\Delta V_g = 0$ V) and asymmetric ($\Delta V_g = -3$ V) confinement potential. For clarity, the conductance trace of the asymmetric QPC is horizontally offset. **b**, The dispersion relation of 1D subbands with SO coupling. When the Fermi energy E_{F} is tuned below the crossing point between the two spin-polarized subbands, both the right- $(+k_x)$ and left-moving $(-k_x)$ electrons are fully spin-polarized which we refer to as the spin-down and spin-up states, respectively. This allows the QPC to acts as a spin injector/detector in the spin FET devices. **c**, The SO-induced spin splitting is further enlarged vertically by the electron-electron (e-e) interaction.

It has recently been suggested[19,20] that the strong electron-electron interaction could further displace these two spin-polarized 1D subbands vertically with respect to each other (Supplementary Fig. 1c), similar to the mechanism which is known to lift the spin degeneracy in GaAs[32−34]. As the edges of the two spin-polarized 1D subbands are no longer at the same energy, a conductance plateau near $0.5(2e^2/h)$ occurs. Although the $0.5(2e^2/h)$ feature was not observed in this work, we do not intend to rule out the possibility of electron-electron interaction in our QPCs, since it is possible that the electron-electron interaction strength γ (and hence the vertical spin splitting) is not large enough to be manifested in QPC conductance at finite temperatures[19,33].

Supplementary Section 2. QPC spin polarization

In order to verify that the QPC indeed acts as spin injector and collector when operated near threshold, we followed the spatial spin separation technique[35] to directly measure the spin content of the current injected from the QPC. A new type of devices, known as magnetic focusing devices (inset of Supplementary Fig. 2), were fabricated on the same wafer as the spin FET devices (see Method Summary). As shown in Ref. 35, in the presence of SO coupling the spin-up and spin-down electrons at the Fermi energy have different momenta when travelling along the same direction. This leads to different cyclotron orbits for the two spin states in a transverse magnetic field, and consequently, a spatial separation of each spin-type of electrons when they are injected from the QPC. The spatial separation of spins is manifested in focusing spectrum, in which the peaks occur when the cyclotron diameter equals the distance, L, between QPC injector and collector (i.e., when the electrons can flow ballistically from the injector into the collector). Since the spin-up and the spin-down electrons have different momenta and are spatially separated when emitted from

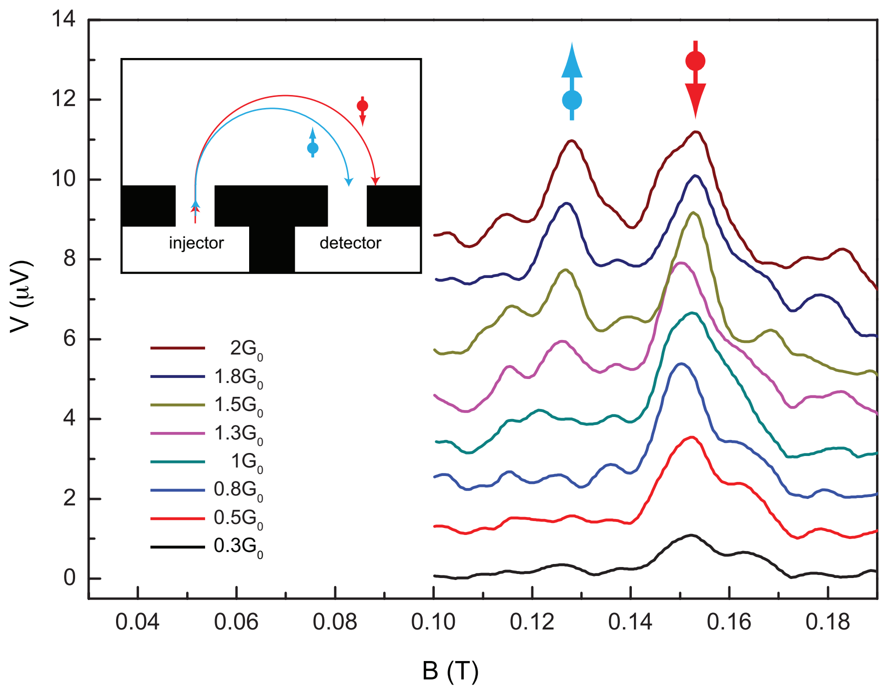

Supplementary Fig. 2: **Magnetic focusing spectrum.** The magnetic focusing spectrum shows the SO-induced doublet when the QPC injector is $\geq 2e^2/h$. The low-field (high-field) peak within the doublet corresponds to the spin-up (spin-down) focusing electrons. The spin-up peak almost vanishes while the spin-down peak still remains when the injector is tuned below $2e^2/h$, indicating that the current injected from the QPC is spin-polarized. The QPC collector is fixed at $\sim 3e^2/h$ to allow both electron spins to pass through, and a constant $100\ \mu$V a.c. voltage is applied across the injector. The data are vertically offset by $1\ \mu$V for clarity. The inset shows the schematic of a magnetic focusing device, where the spin-up and spin-down currents emitted from the QPC injector are spatially separated in the presence of SO coupling, which results in the observation of spin-resolved focusing peaks.

the QPC injector, the spin-up and spin-down focusing peaks appear at different magnetic fields $B_{\uparrow\downarrow} = 2p_{\uparrow\downarrow}/eL$, where $p_{\uparrow}$ and $p_{\downarrow}$ are momenta for spin-up and spin-down electrons.

Supplementary Fig. 2 shows the focusing voltage as a function of a weak transverse magnetic field. In this measurement, the central gate was held at -2.9 V while the left-hand arm of the QPC injector was varied between -1.6 and -2.2 V to tune the conductance from $2G_0$ to $0.3G_0$ (where $G_0 = 2e^2/h$). When the QPC injector is tuned to high conductance values, the focusing peak doublets are present, where the high-field and low-field peak corresponds to the spin-down and spin-up focusing electrons, respectively. This shows that the injected current contains both electron spins. The height of the spin-up peak gradually reduces with decreasing the conductance. The spin-up peak vanishes while the spin-down peak still remains when the injector is tuned below $2e^2/h$, indicating[35] that the current injected from the QPC contains only the spin-down electrons and is indeed spin-polarized. A separate and direct measurement of the QPC spin polarization reported here confirms that the QPC indeed acts as spin injector/detector and furthermore substantiate the results presented in the main article. Note that the peak separation can also be used to estimate the SO coupling constant[35], giving $|\alpha| \sim 20 \times 10^{-12}$ eVm.

Supplementary Section 3. Derivation of the spin precession

In this work, the spin precession is driven by the Rashba SO coupling and an external magnetic field along the y-direction, of which the contributions to the Hamiltonian are $H_{\rm SO} = \alpha(-k_x\sigma_y + k_y\sigma_x)$ and $H_{\rm Z} = g\mu_{\rm B}B_{\rm ext}\sigma_y/2$ (where $\sigma_{x,y}$ are Pauli matrices), respectively. As mentioned in the main article, the use of QPCs as the spin injector and detector in the spin FET restricts the transport channel to be quasi-1D and thus sets $k_y = 0$ in the Rashba term.

The time evolution of the spinors moving in the semiconductor channel is given by

$$|\chi(t)\rangle = e^{-i(H_{\mathrm{SO}}+H_{\mathrm{Z}})t/\hbar}\,|\chi(0)\rangle = e^{i\omega_{\mathrm{L}}\sigma_y t/2}\,|\chi(0)\rangle\,, \tag{1}$$

where $\omega_{\mathrm{L}} = (2\alpha k_x - g\mu_{\mathrm{B}}B_{\mathrm{ext}})/\hbar$. As the QPC injector is polarized in the z-direction, the spin state of electrons launched from the QPC is given by $|\chi(0)\rangle = \begin{pmatrix} 1 \\ 0 \end{pmatrix}$ on the Bloch sphere, which evolves to

$$|\chi(t)\rangle = \begin{pmatrix} \cos\frac{\omega_{\mathrm{L}}t}{2} & \sin\frac{\omega_{\mathrm{L}}t}{2} \\ -\sin\frac{\omega_{\mathrm{L}}t}{2} & \cos\frac{\omega_{\mathrm{L}}t}{2} \end{pmatrix}\begin{pmatrix} 1 \\ 0 \end{pmatrix} = \begin{pmatrix} \cos\frac{\omega_{\mathrm{L}}t}{2} \\ -\sin\frac{\omega_{\mathrm{L}}t}{2} \end{pmatrix}. \tag{2}$$

It is clear that the Rashba and Zeeman terms of the Hamiltonian cause the electron spin to precess about the y-axis with a frequency ω_{L}. With $t = Lm^*/\hbar k_x$ (where L is the distance between the QPC injector and detector, and m^* is the electron's effective mass), we are able to obtain the precession angle

$$\Delta\theta = \omega_{\mathrm{L}}t = 2m^*\alpha L/\hbar^2 - g\mu_{\mathrm{B}}B_{\mathrm{ext}}m^*L/k_x\hbar^2. \tag{3}$$

Supplementary Section 4. InGaAs quantum well

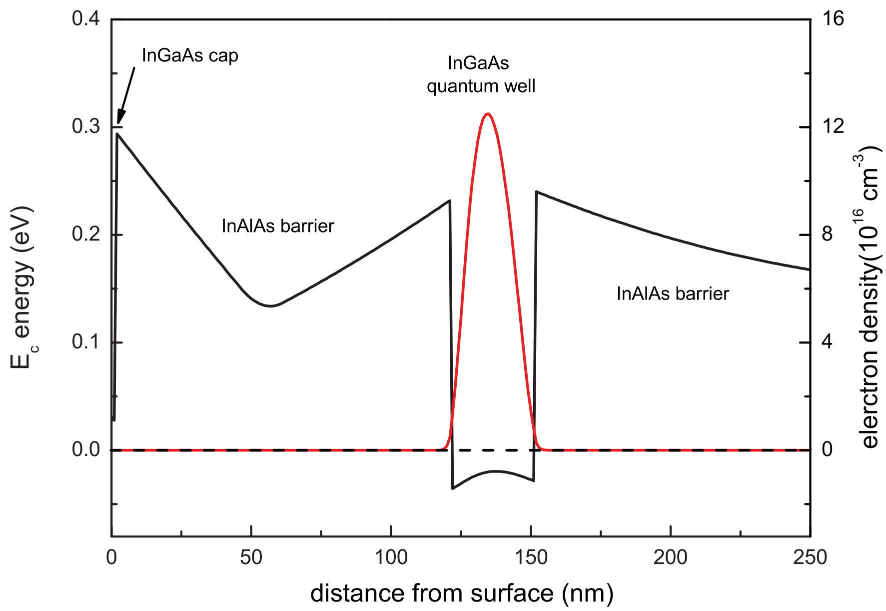

Supplementary Fig. 3: **Conduction band profile.** Conduction band profile and electron density for the InGaAs quantum well, calculated using Snider's "1D POISSON/SCHRODINGER" program (Ref. 36).

References

19. Debray, P. *et al.* All-electric quantum point contact spin-polarizer. *Nature Nanotechnology* **4**, 759-764 (2009).

20. Wan, J., Cahay, M., Debray, P. & Newrock, R. Possible origin of the 0.5 plateau in the ballistic conductance of quantum point contacts. *Phys. Rev. B* **80**, 155440 (2009).

21. Quay, C. H. L. *et al.* Observation of a one-dimensional spin-orbit gap in a quantum wire. *Nature Physics* **6**, 336-339 (2010).

25. Moroz, A. V. & Barnes, C. H. W. Effect of the spin-orbit interaction on the band structure and conductance of quasi-one-dimensional systems. *Phys. Rev. B* **60**, 14272 (1999).

32. Wang, C.-K. & Berggren, K.-F. Spin splitting of subbands in quasi-one-dimensional electron quantum channels. *Phys. Rev. B* **54**, R14257 (1996).

33. Lassl, A., Schlagheck, P. & Richter, K. Effects of short-range interactions on transport through quantum point contacts: A numerical approach. *Phys. Rev. B* **75**, 045346 (2007).

34. Graham, A. C., Sawkey, D. L., Pepper, M., Simmons, M. Y. & Ritchie, D. A. Energy-level pinning and the 0.7 spin state in one dimension: GaAs quantum wires studied using finite-bias spectroscopy. *Phys. Rev. B* **75**, 035331 (2007).

35. Rokhinson, L. P., Larkina, V., Lyanda-Geller, Y. B., Pfeiffer, L. N. & West, K. W. Spin separation in cyclotron motion. *Phys. Rev. Lett.* **93**, 146601 (2004).

36. Snider, G. 1D POISSON/SCHRODINGER program. http://www3.nd.edu/ gsnider/